UDC 621.314 https://doi.org/10.20998/2074-272X.2026.3.11

A. Ahmane, D. Sakri, S.E. Farhi, N. Golea

Three-phase pulse width modulation boost rectifier enhancement direct power control based on super-twisting algorithm

Introduction. *Three-phase pulse width modulation (PWM) rectifiers are widely used in modern power conversion systems due to their high efficiency, controllability, and ability to provide high-quality energy conversion. They play a crucial role in applications such as motor drives, renewable energy integration, and power supplies, where a stable DC voltage and low harmonic distortion are essential. The conventional direct power control (DPC) method, based on a 12-sector switching table, is commonly employed for its simple implementation, reduced complexity, and fast dynamic response*. ***Problem.*** *Despite its simplicity and fast dynamic response, the classical DPC approach is highly sensitive to parameter variations and relies on a predefined switching table, which limits its robustness and current quality.* ***Goal****. To experimentally validate an improved control strategy for a three-phase PWM rectifier that enhances robustness and current quality by integrating the super-twisting algorithm (STA) into the conventional DPC framework.* ***Methodology****. The proposed STA-based DPC was implemented and tested on an experimental setup using a dSPACE DS1104 digital control board. Both the conventional DPC and the modified STA-based DPC were experimentally evaluated under the same operating conditions to ensure fair comparison.* ***Results.*** *Experimental results demonstrate that the STA-based DPC achieves a THD reduction from 11.85 % to 6.11 % and improves the stability of the DC-link voltage under parameter variations. These quantitative results confirm current quality, improved robustness and reduced chattering compared to the classical DPC.* ***Scientific novelty.*** *Integrating the STA into the DPC framework eliminates dependence on the predefined switching table and enhances robustness to system uncertainties.* ***Practical value.*** *The experimental validation confirms the feasibility and effectiveness of implementing the STA-based DPC in real-time applications, offering a reliable and high-performance solution for modern power conversion systems.* References 17, tables 4, figures 19.
Key words: **direct power control, sliding mode control, super twisting algorithm, three-phase PWM rectifier, dSPACE 1104.**

Вступ*. Трифазні випрямлячі з ШІМ (PWM) широко застосовуються в сучасних системах перетворення енергії завдяки їх високій ефективності, керованості та здатності забезпечувати високу якість електроенергії. Вони відіграють важливу роль у таких застосуваннях, як електроприводи, інтеграція відновлюваних джерел енергії та системи живлення, де необхідні стабільна напруга постійного струму та низький рівень гармонічних спотворень. Традиційний метод прямого керування потужністю (DPC), заснований на 12-секторній таблиці перемикання, широко застосовується завдяки простоті реалізації, зниженій складності та високій швидкодії.* ***Проблема****. Незважаючи на простоту та швидку динамічну реакцію, класичний підхід DPC є чутливим до варіацій параметрів і базується на заздалегідь визначеній таблиці перемикання, що обмежує його робастність і якість струму.* ***Мета****. Експериментально підтвердити ефективність удосконаленої стратегії керування трифазним PWM-випрямлячем, яка підвищує робастність і якість струму шляхом інтеграції алгоритму суперскручування (STA) у структуру класичного DPC.* ***Методика****. Запропонований підхід DPC на основі STA реалізовано та досліджено на експериментальному стенді з використанням плати цифрового керування dSPACE DS1104. Як класичний DPC, так і модифікований DPC на основі STA експериментально оцінювалися за однакових умов роботи для забезпечення коректного порівняння.* ***Результати****. Експериментальні результати показали, що DPC на основі STA забезпечує зниження коефіцієнта гармонічних спотворень (THD) з 11,85 % до 6,11 % та покращує стабільність напруги в ланці постійного струму за умов зміни параметрів. Отримані результати підтверджують покращення якості струму, підвищення робастності та зменшення тремтіння порівняно з класичним DPC.* ***Наукова новизна****. Інтеграція STA в структуру DPC усуває залежність від заздалегідь визначеної таблиці перемикання та підвищує робастність до невизначеностей системи.* ***Практична значимість****. Експериментальна валідація підтверджує доцільність і ефективність реалізації DPC на основі STA в системах реального часу, що забезпечує надійне та високоефективне рішення для сучасних систем перетворення електроенергії.* Бібл. 17, табл. 4, рис. 19.
Ключові слова: **пряме керування потужністю, керування в ковзному режимі, алгоритм суперскручування, трифазний ШІМ випрямляч, dSPACE 1104.**

Introduction. The control of three-phase pulse width modulation (PWM) boost rectifiers is a key challenge in modern power electronics, particularly for applications that require high energy efficiency and fast dynamic response. Among the various available control strategies, direct power control (DPC) has established itself as an effective solution due to its ability to regulate both active and reactive power without relying on complex modulation techniques [1, 2]. The classical version of DPC is widely adopted for its straightforward implementation and satisfactory dynamic performance [3]. However, this approach also exhibits certain limitations, including steady-state power oscillations and increased sensitivity to parameter variations, which can degrade its performance in practical operating conditions [2].

To overcome these drawbacks an improved version, known as super twisting algorithm-based direct power control (STA-DPC), is proposed. This approach leverages the super twisting sliding mode control (STA-SMC) algorithm to enhance robustness against external disturbances and to significantly mitigate the chattering effect commonly associated with sliding mode control techniques [4, 5]. Unlike the conventional DPC, which relies on fixed switching tables, STA-DPC exclusively uses real-time current and voltage measurements to compute and regulate power, ensuring a more stable and adaptive control process [3, 4].

The main objective of this paper is to experimentally validate, using a dSPACE1104-based digital control platform, the DPC strategy in both its conventional form and the optimized version incorporating the STA. The study aims to compare the performance of both approaches in terms of regulation quality, robustness, and total harmonic distortion (THD) reduction. The expected results demonstrate the benefits of integrating sliding mode control to enhance the performance of three-phase PWM boost rectifiers and open new perspectives for developing more advanced and reliable power converter control strategies [6].

The **goal** of this work is to experimentally validate an improved control strategy for a three-phase PWM rectifier that enhances robustness and current quality by integrating the super-twisting algorithm (STA) into the conventional DPC framework.

Topology and modeling of a three-phase boost PWM rectifier. For modeling purposes, the equivalent single-phase electrical circuit is shown in Fig. 1.

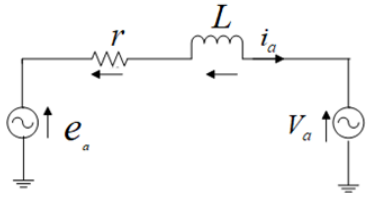

Fig. 1. Per-phase electrical circuit model of the PWM rectifier

Based on the per-phase equivalent circuit in Fig. 1, the AC-side equations for all 3 phases are given by:

$$\begin{cases} L\dfrac{\mathrm{d}i_a}{\mathrm{d}t} = e_a - ri_a - V_a; \\ L\dfrac{\mathrm{d}i_b}{\mathrm{d}t} = e_b - ri_b - V_b; \\ L\dfrac{\mathrm{d}i_c}{\mathrm{d}t} = e_c - ri_c - V_c, \end{cases} \tag{1}$$

where i_a, i_b, i_c are the 3-phase grid currents; e_a, e_b, e_c are the 3-phase grid voltages; V_a, V_b, V_c are the controllable bridge converter voltage, regulated from the DC side; r is the resistance of the interconnecting filters; L is the inductance of the interconnecting filters.

The topology of the 3-phase PWM rectifier is illustrated in Fig. 2 [7, 8].

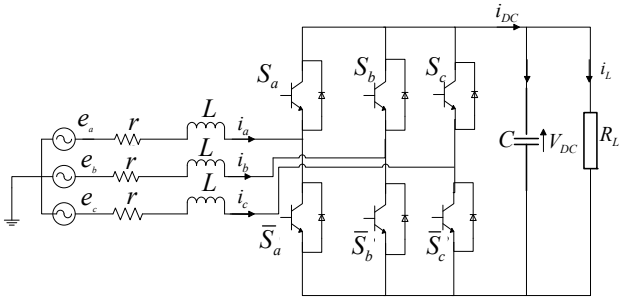

Fig. 2. Three-phase PWM rectifier electrical circuit

According to (1) and Fig. 2, a 3-phase PWM rectifier equation is given as follows [7, 8]:

$$\begin{cases} L\dfrac{\mathrm{d}i_a}{\mathrm{d}t} = e_a - ri_a - \dfrac{V_{DC}}{3}(2S_a - S_b - S_c); \\ L\dfrac{\mathrm{d}i_b}{\mathrm{d}t} = e_b - ri_b - \dfrac{V_{DC}}{3}(-S_a + 2S_b - S_c); \\ L\dfrac{\mathrm{d}i_c}{\mathrm{d}t} = e_c - ri_c - \dfrac{V_{DC}}{3}(-S_a - S_b + 2S_c); \\ C\dfrac{\mathrm{d}V_{DC}}{\mathrm{d}t} = (S_a i_a + S_b i_b + S_c i_c) - \dfrac{V_{DC}}{R_L}, \end{cases} \tag{2}$$

where: V_{DC} is the DC link voltage; R_L is the load resistance on the DC side; C is the capacitance on the DC side; S_a, S_b, S_c are the control signals.

Using the Park transformation, the PWM rectifier equations expressed in the stationary a, b, c frame are converted into the synchronous d-q frame for simplified analysis [9]:

$$\begin{cases} L\dfrac{\mathrm{d}i_d}{\mathrm{d}t} = e_d - ri_d + \omega L i_q + V_d; \\ L\dfrac{\mathrm{d}i_q}{\mathrm{d}t} = e_q - ri_q + \omega L i_d + V_q; \\ C\dfrac{\mathrm{d}V_{DC}}{\mathrm{d}t} = S_d i_d + S_q i_q - \dfrac{V_{DC}}{R_L}, \end{cases} \tag{3}$$

where $V_d = \neg S_d V_{DC}$; $V_q = \neg S_q V_{DC}$; i_d, i_q are the grid currents in d-q reference frame; e_d, e_q are the grid voltages in d-q reference frame; V_d, V_q are the controllable bridge converter voltage, regulated from the DC side in d-q reference frame.

The source delivers both active P and reactive Q powers, which are defined as:

$$\begin{aligned} P &= \mathrm{Re}\{\underline{u}\cdot\underline{i}^*\} = e_a i_a + e_b i_b + e_c i_c; \\ P &= e_\alpha i_\alpha + e_\beta i_\beta; \end{aligned} \tag{4}$$

$$\begin{aligned} Q &= \mathrm{Im}\{\underline{u}\cdot\underline{i}^*\} = \frac{1}{\sqrt{3}}(e_a i_a + e_b i_b + e_c i_c); \\ Q &= e_\beta i_\alpha + e_\alpha i_\beta. \end{aligned} \tag{5}$$

It gives in the synchronous d-q coordinates:

$$\begin{aligned} P &= e_d i_d + e_q i_q; \\ Q &= e_q i_d + e_d i_q. \end{aligned} \tag{6}$$

Direct power control (DPC) is an advanced control technique implemented on 3-phase converters employing PWM to regulate active and reactive power flows, this method relies on the instantaneous measurement of phase voltages and currents, from which the active and reactive powers are determined in real time [10, 11].

The computed power values are then continuously compared with their respective reference values. The resulting error signals are processed by hysteresis regulators, which determine the appropriate voltage vector components, typically within the stationary $\alpha\beta$ reference frame. Based on these control variables, a switching table is utilized to generate the required gating signals for the converter switches, thereby ensuring fast and accurate power regulation (Fig. 3) [3, 7, 8].

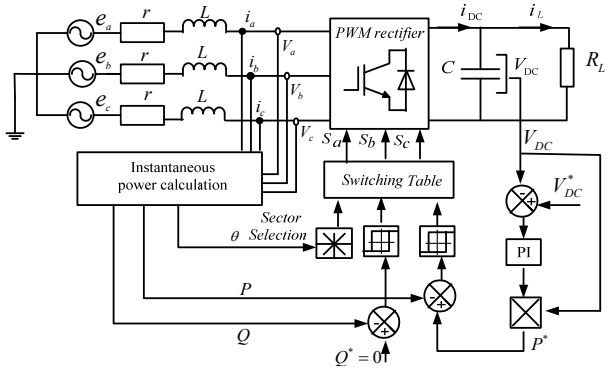

Fig. 3. DPC scheme

The angular region of the voltage (or flux) vector is divided into 12 sectors, which can be numerically indexed as:

$$(n-1)\frac{\pi}{6} \le \theta < n\frac{\pi}{6}, \tag{7}$$

where n is the sector number, ranging from 1 to 12; $\theta \in [0; 2\pi]$ is the voltage vector position obtained as:

$$\theta = \mathrm{arctg}(V_\beta / V_\alpha). \tag{8}$$

Table 1 defines the switching logic used in the DPC scheme to generate the inverter switching signals. The table receives 3 inputs: the outputs of the hysteresis comparators for the active and reactive power errors (d_p and d_q), and the sector angle θ that indicates the position of the reference voltage vector in the α, β plane. Based on the combination of these inputs, the corresponding voltage vector (V_0–V_7) is selected from the table. Each voltage vector represents a specific switching state of the inverter, determining which semiconductor devices are turned on or off. In this way, the table translates the instantaneous power errors and the sector location into the appropriate switching commands, ensuring fast and accurate control of active and reactive power.

Table 1

Switching table for DPC

d_p	1	1	0	0
d_q	0	1	0	1
θ_1	V_6	V_7	V_1	V_2
θ_2	V_0	V_0	V_1	V_2
θ_3	V_1	V_0	V_2	V_3
θ_4	V_7	V_7	V_2	V_3
θ_5	V_2	V_7	V_3	V_4
θ_6	V_0	V_0	V_3	V_4
θ_7	V_3	V_0	V_4	V_5
θ_8	V_7	V_7	V_4	V_5
θ_9	V_4	V_7	V_5	V_6
θ_{10}	V_0	V_0	V_5	V_6
θ_{11}	V_5	V_0	V_6	V_1
θ_{12}	V_7	V_7	V_6	V_1

Experimental validation of classical DPC. While simulation alone cannot capture all real-world physical phenomena – such as measurement errors, delays, data processing times and noise – real-time implementation of control techniques is essential for evaluating algorithm performance under practical conditions. In this section, the classical DPC scheme, which integrates a PI regulator for DC-link voltage regulation and hysteresis controllers for active and reactive power, is validated experimentally using a dSPACE 1104 card. The objective is to assess its real-time behavior on an experimental test bench developed in our LGEA laboratory. The experimental tests were conducted according to Fig. 4, which presents the experimental setup and highlights the main devices used for validation. The detailed list and specifications of these components are provided in Table 2, ensuring accurate measurements and effective control throughout the experiments.

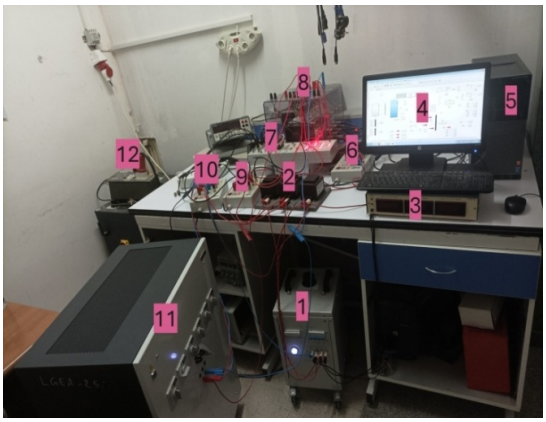

Fig. 4. DPC experimental validation

Table 2

The devices list of DPC experimental tests

Number	Name
1	3-phase autotransformer
2	3-phase inductor
3	Ammeter
4	Simulink and ControlDesk
5	PC unit includes a DS1104 card
6	Interface card
7	Control panel CLP 1104
8	SEMIKRON inverter
9	Current sensors
10	Voltage sensors
11	DC variable load
12	3-phase AC supply

The main parameters of the 3-phase PWM rectifier used in the simulations are summarized in Table 3.

Table 3

Parameters of 3-phase PWM rectifier

Parameters	Value
Grid voltage, V	120
Reference of DC-link voltage V^*_{DC}, V	300
Grid line inductance L, mH	10
Grid line resistance r, Ω	0.1
DC-link capacitor C, μF	1100
Load resistance R_L, Ω	80 → 50
Grid frequency f, Hz	50

Two experiments are carried out to evaluate the performance of the proposed control scheme under different operating conditions.

Test 1. In the first experiment, the DC-link voltage was kept constant at 200 V, while the load resistance was decreased from 80 Ω to 50 Ω. The waveforms of the different variables obtained via ControlDesk are displayed in Fig. 5–8. Figure 5 shows that the DC-link voltage accurately tracks its reference without being affected by load variations, demonstrating that the regulator provides a fast dynamic response and ensures voltage stability despite transient fluctuations in load power.

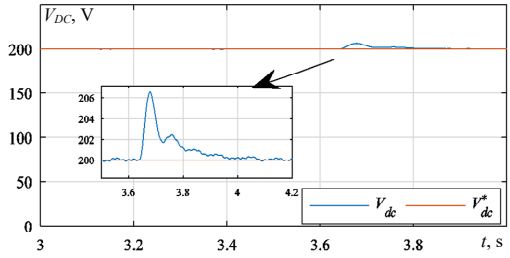

Fig. 5. DC-link voltage

Figure 6 shows the active power, demonstrating its ability to accurately track its reference even during load variations; when the load changes at 3.6 s, the active power continues to follow its setpoint, highlighting the system's fast response and strong dynamic performance.

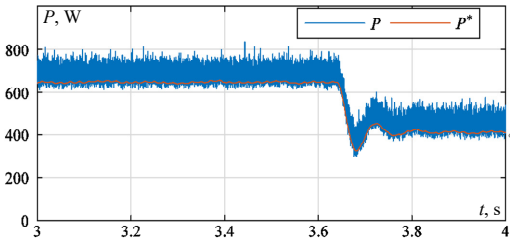

Fig. 6. Active power and its reference

Figure 7 shows the reactive power and its reference, indicating that the reactive power remains at zero throughout the transient period, thereby confirming that a unity power factor is maintained.

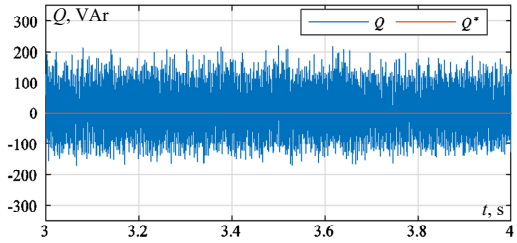

Fig. 7. Reactive power and its reference

Figure 8 presents, on the same graph, the current and voltage waveforms of the first grid phase. Both waveforms are sinusoidal and in phase, indicating operation at a unity power factor.

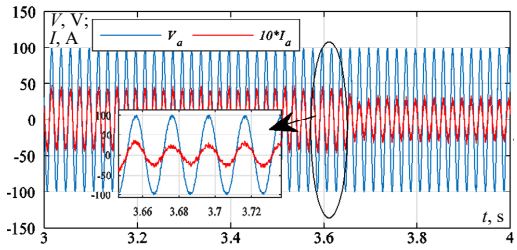

Fig. 8. Input voltage and current for the rectifier

Test 2. In the second experiment, the load resistance was kept constant at 80 Ω, while the DC-link voltage was reduced from 250 V to 200 V. Figures 9–11 show the results of the second test. The analysis of the waveforms yields the following comments:

- The DC-link voltage constantly tracks its reference profile.
- The active power clearly follows the generated reference with high accuracy, reflecting the applied load variations.
- The reactive power maintains a zero average value under varying load conditions, thereby ensuring unity power factor operation.

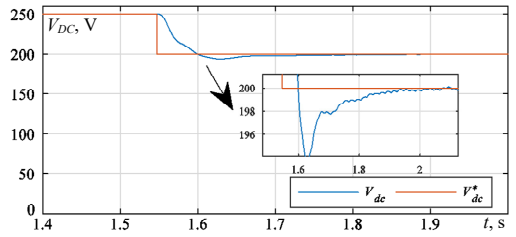

Fig. 9. DC link voltage and his reference

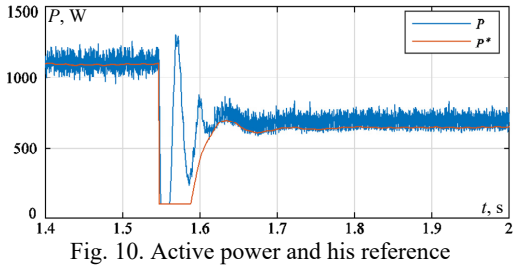

Fig. 10. Active power and his reference

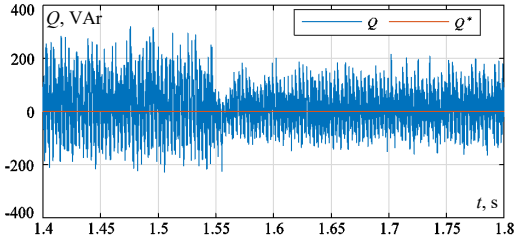

Fig. 11. Reactive power and his reference

Super twisting direct power control. The super-twisting sliding mode control (STA-SMC) is a robust nonlinear control strategy that has proven highly effective in enhancing the dynamic performance of 3-phase PWM rectifiers (Fig. 12). These rectifiers are widely employed in industrial applications to convert AC into DC while maintaining a high power factor, minimizing THD, and enabling bidirectional power flow [12, 13].

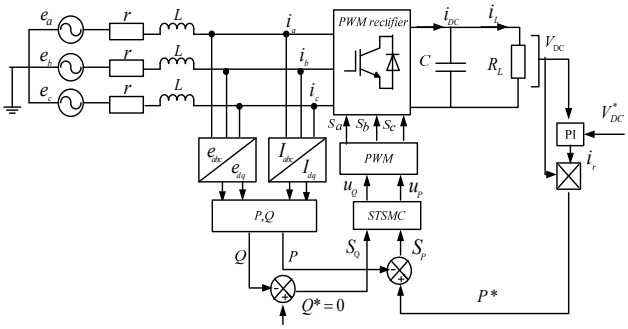

Fig. 12. STA-DPC scheme

The implementation of STA-SMC provides an effective solution for enhancing the dynamic performance of 3-phase PWM rectifiers, owing to its inherent robustness, high precision, and capability to mitigate chattering effects [14, 15]. These characteristics make it particularly well suited for applications in renewable energy systems, industrial automation, and electric vehicle charging stations. However, its practical deployment presents 2 major challenges: first, its complex design requires careful tuning of parameters, such as sliding surface coefficients and control gains, to achieve an optimal trade-off between performance and robustness; second, it involves significant computational demands, as real-time implementation requires solving nonlinear equations, which often necessitates the use of advanced digital signal processors (DSPs) [6, 15].

The STA-SMC law u_{ST} is composed of two components [16, 17]. The first component is represented by its time derivative $u_1(t)$, while the second component is determined as a function of the sliding variable $u(t)$. The STA control law is expressed as [12]:

$$u_{ST} = u(t) + u_1(t), \tag{9}$$

with:

$$\begin{cases} u = -\lambda |S|^{\rho} \operatorname{sign}(S); \\ \dot{u}_1 = \alpha \operatorname{sign}(S), \end{cases}$$

where α, $\lambda > 0$ that are used to regulate the STA; ρ is the parameter used to adjust the degree of non-linearity, where $0 < \rho < 0.5$.

To perform maximum second-order SMC, ρ is often set to 0.5. The law STSMC for the power controller is defined by:

$$\begin{cases} u_{ST} = -\lambda |S|^{0.5} \operatorname{sign}(S) + u_1; \\ \dot{u}_1 = \alpha \operatorname{sign}(S). \end{cases} \quad (10)$$

In (10), $\lambda = \sqrt{u}$ and $\alpha = 1.1u$, where $u > 0$ with sufficiently large value. Here, the power errors $e_1 = P_{ref} - P$ and $e_2 = Q_{ref} - Q$ are chosen as the sliding surfaces. This approach is based on the STA without an equivalent control term. The stability proof of this control strategy and the convergence of the states can be found in [14].

Experimental validation of STA-DPC. For this control strategy based on the STA algorithm, two test scenarios are considered: first, a variation of the load resistance between 50 Ω and 80 Ω while maintaining a constant DC bus voltage; then, an increase in the DC bus reference voltage with the load resistance fixed at 80 Ω. The measured variables acquired via ControlDesk are illustrated by curves in Fig. 13–19.

Test 1 (load resistance variation). Unlike the first conventional DPC control technique; this experimental test consists in increasing the load to 80 Ω within the interval [6 s, 16 s] in order to observe the behavior of the different variables. The analysis of these variables allows us to make the following remarks:

- The DC bus voltage perfectly tracks its reference with excellent disturbance rejection in response to the load variation at 6 s and 16 s.
- The active power provided by the electrical grid adjusts to meet the load demand: it decreases when the load increases and accurately tracks its reference. Meanwhile, the reactive power maintains a zero average value, which improves the quality of the supplied energy and ensures that the current remains in phase with the grid voltage (Fig. 16).
- The voltage remains purely sinusoidal with fixed amplitude, while the currents preserve a sinusoidal waveform whose amplitude varies in accordance with load fluctuations.

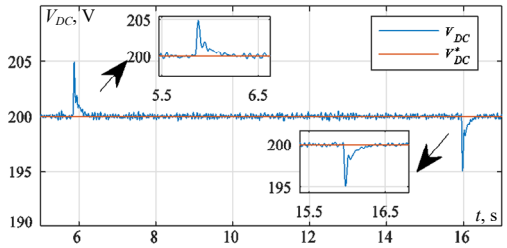

Fig. 13. DC-link voltage

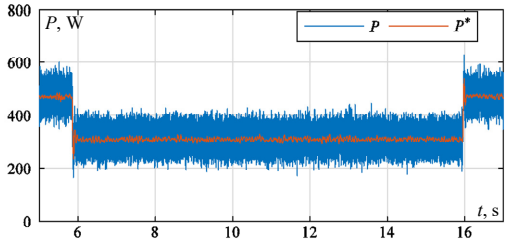

Fig. 14. Active power and its reference

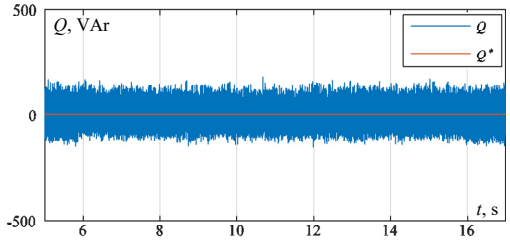

Fig. 15. Reactive power and its reference

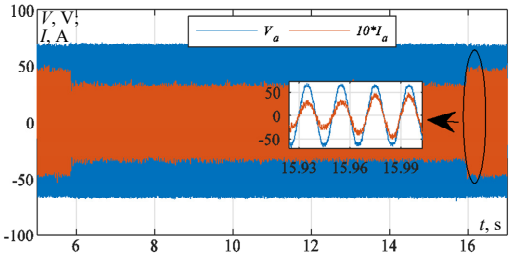

Fig. 16. Input voltage and current for the rectifier

Test 2. DC-link reference voltage increase. In this second test, the load resistance was kept constant at 80 Ω, while the DC-link reference voltage was increased from 180 V to 200 V. Figures 17–19 illustrate the corresponding results:

- The DC-link voltage consistently follows its reference profile.
- The active power accurately tracks the generated reference, clearly reflecting the applied load conditions.
- The reactive power remains zero on average, even under DC-link voltage variations, thereby guaranteeing operation at unity power factor.

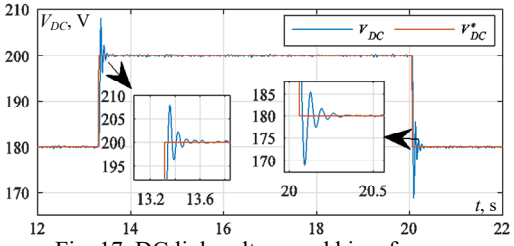

Fig. 17. DC link voltage and his reference

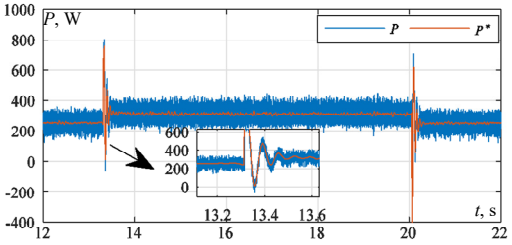

Fig. 18. Active power and its reference

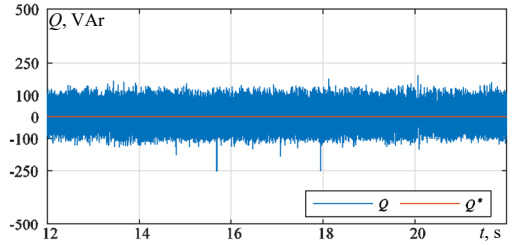

Fig. 19. Reactive power and its reference

In the practical tests, when the STA-DPC strategy was implemented in Test 1 (with load variation), the THD

dropped to 6.11 %, compared to 11.85 % with the classical DPC (Table 4). This significant reduction demonstrates the superior capability of the STA-DPC approach to minimize harmonics and improve current quality.

In Test 2 (the DC-link voltage varied) the classical DPC recorded a THD of 10.21 %, whereas the STA-DPC achieved a slightly lower value of 9.7 %. Although the improvement is less substantial than in the variable load scenario, it still confirms the enhanced harmonic mitigation performance of the STA-DPC method.

It is worth noting that the limited accuracy of the current and voltage sensors may have adversely affected the measurements. Under ideal sensing conditions, even better THD performance could likely be achieved.

Table 4

THD value

Strategy	DC-link voltage variation	Load variation
DPC	10.21 %	11.85 %
STA-DPC	9.7 %	6.11 %

Conclusions. This study experimentally validated an improved control strategy for a 3-phase PWM rectifier by integrating the STA into the conventional DPC framework.

The experimental implementation on a DSP-1104 platform demonstrated that the proposed DPC-STA approach significantly enhances system robustness, dynamic response, and current quality compared to the classical DPC method. In particular, the reduction of THD from 11.85 % to 6.11 % confirms the effectiveness of the proposed method in improving current waveform quality and ensuring stable DC-link regulation under parameter variations.

Beyond validating the control performance, this work confirms the feasibility of implementing second-order sliding mode techniques in real-time power converter applications. Future research will focus on extending this approach to grid-connected converters and renewable energy interfaces to further exploit its robustness and control accuracy.

Conflict of interest. The authors declare that they have no conflicts of interest.

REFERENCES

1. Escobar G., Stankovic A.M., Carrasco J.M., Galvan E., Ortega R. Analysis and design of direct power control (DPC) for a three phase synchronous rectifier via output regulation subspaces. *IEEE Transactions on Power Electronics*, 2003, vol. 18, no. 3, pp. 823-830. doi: https://doi.org/10.1109/TPEL.2003.810862.

2. Ouchen S., Abdeddaim S., Betka A., Menadi A. Experimental validation of sliding mode-predictive direct power control of a grid connected photovoltaic system, feeding a nonlinear load. *Solar Energy*, 2016, vol. 137, pp. 328-336. doi: https://doi.org/10.1016/j.solener.2016.08.031.

3. Liu Z. A review of Direct Power Control Technologies for Three-Phase Voltage PWM Rectifiers. *Science and Technology of Engineering, Chemistry and Environmental Protection*, 2024, vol. 2, no. 7, pp. 1-5. doi: https://doi.org/10.61173/h3f6e192.

4. Fekik A., Hamida M.L., Denoun H., Sambas A., Vaidyanathan S., Abdurrahman U.T., Mujiarto. Super-twisting sliding mode direct power control of PWM-rectifier connected to grid. *AIP Conference Proceedings*, 2023, vol. 2510, no. 1, art. no. 020002. doi: https://doi.org/10.1063/5.0128272.

5. Mazouz F., Belkacem S. *Super Twisting Algorithm Direct Power Control of DFIG Using Space Vector Modulation*. 2021. 6 p. doi: https://doi.org/10.20944/preprints202007.0628.v2.

6. Benbouhenni H., Yessef M., Bizon N., Bossoufi B., Alghamdi T.A.H. Experimental Assessment of a Dual Super-Twisting Control Technique of Variable-Speed Multi-Rotor Wind Turbine Systems. *IEEE Access*, 2024, vol. 12, pp. 103744-103763. doi: https://doi.org/10.1109/ACCESS.2024.3434534.

7. Hou B., Qi J., Li H. Robust Direct Power Control of Three-Phase PWM Rectifier with Mismatched Disturbances. *Electronics*, 2024, vol. 13, no. 8, art. no. 1476. doi: https://doi.org/10.3390/electronics13081476.

8. Krylov D.S., Kholod O.I. Determination of the input filter parameters of the active rectifier with a fixed modulation frequency. *Electrical Engineering & Electromechanics*, 2022, no. 4, pp. 21-26. doi: https://doi.org/10.20998/2074-272X.2022.4.03.

9. Harrabi N., De Almeida J.S., Laboudi K. Controller Design Approach for SVPWM-Regulated AC/DC Rectifier. *European Journal of Electrical Engineering*, 2021, vol. 23, no. 5, pp. 353-360. doi: https://doi.org/10.18280/ejee.230501.

10. Barkat S., Tlemcani A., Nouri H. Direct power control of the PWM rectifier using sliding mode control. *International Journal of Power and Energy Conversion*, 2011, vol. 2, no. 4, art. no. 289. doi: https://doi.org/10.1504/IJPEC.2011.041883.

11. Sakri D., Laib H., Farhi S.E., Golea N. Sliding mode approach for control and observation of a three phase AC-DC pulse-width modulation rectifier. *Electrical Engineering & Electromechanics*, 2023, no. 2, pp. 49-56. doi: https://doi.org/10.20998/2074-272X.2023.2.08.

12. Ahmane A., Sakri D., Golea N. Direct Power Control based on Super Twisting Sliding Mode Control for Three Phase PWM Rectifier. *2022 2nd International Conference on Advanced Electrical Engineering (ICAEE)*, 2022, pp. 1-6. doi: https://doi.org/10.1109/ICAEE53772.2022.9962104.

13. Dekali Z., Baghli L., Boumediene A. Improved Super Twisting Based High Order Direct Power Sliding Mode Control of a Connected DFIG Variable Speed Wind Turbine. *Periodica Polytechnica Electrical Engineering and Computer Science*, 2021, vol. 65, no. 4, pp. 352-372. doi: https://doi.org/10.3311/PPee.17989.

14. Ouchen S., Benbouzid M., Blaabjerg F., Betka A., Steinhart H. Direct Power Control of Shunt Active Power Filter Using Space Vector Modulation Based on Supertwisting Sliding Mode Control. *IEEE Journal of Emerging and Selected Topics in Power Electronics*, 2021, vol. 9, no. 3, pp. 3243-3253. doi: https://doi.org/10.1109/JESTPE.2020.3007900.

15. Zeb K., Busarello T.D.C., Ul Islam S., Uddin W., Raghavendra K.V.G., Khan M.A., Kim H.-J. Design of Super Twisting Sliding Mode Controller for a Three-Phase Grid-connected Photovoltaic System under Normal and Abnormal Conditions. *Energies*, 2020, vol. 13, no. 15, art. no. 3773. https://doi.org/10.3390/en13153773.

16. Oualah O., Kerdoun D., Boumassata A. Super-twisting sliding mode control for brushless doubly fed reluctance generator based on wind energy conversion system. *Electrical Engineering & Electromechanics*, 2023, no. 2, pp. 86-92. doi: https://doi.org/10.20998/2074-272X.2023.2.13.

17. Yenil V., Özdemir S., Ortatepe Z. Super Twisting Sliding Mode Control of Four-Phase Interleaved Boost Converter. *Gazi University Journal of Science Part A: Engineering and Innovation*, 2024, vol. 11, no. 3, pp. 563-576. doi: https://doi.org/10.54287/gujsa.1529271.

Received 02.10.2025
Accepted 10.12.2025
Published 02.05.2026

A. Ahmane[1], *PhD Student,*
D. Sakri [1], *Doctor of Electrotechnical, Professor,*
S.E. Farhi [1,2], *Doctor of Electrotechnical, Professor,*
N. Golea [1], *Doctor of Electrotechnical, Professor,*
[1] Laboratory of Electrical Engineering and Automatic (LGEA), University of Oum El Bouaghi, Algeria,
e-mail: anissa.ah93@gmail.com (Corresponding Author)
[2] Department of Electrical Engineering, University of Souk Ahras, Algeria.

How to cite this article:
Ahmane A., Sakri D., Farhi S.E., Golea N. Three-phase pulse width modulation boost rectifier enhancement direct power control based on super-twisting algorithm. *Electrical Engineering & Electromechanics*, 2026, no. 3, pp. 73-78. doi: https://doi.org/10.20998/2074-272X.2026.3.11